ORIGINAL RESEARCH

Blood Coral Polysaccharide Helps Prevent D-Gal/LPS-Induced Acute Liver Failure in Mice

Chong Li[1,2,]*, Shu Lai[3,]*, Ruokun Yi[1], Xianrong Zhou[1,2], Xin Zhao [1], Qiang Li[4]

[1]Collaborative Innovation Center for Child Nutrition and Health Development, Chongqing Engineering Research Center of Functional Food, Chongqing Engineering Laboratory for Research and Development of Functional Food, Chongqing University of Education, Chongqing, People's Republic of China; [2]Department of Food and Nutrition, College of Medical and Life Science, Silla University, Busan, Republic of Korea; [3]Department of Pharmacology, Jiulongpo District People's Hospital of Chongqing, Chongqing, People's Republic of China; [4]Department of Emergency, The First Affiliated Hospital of Gannan Medical College, Ganzhou, Jiangxi, People's Republic of China

*These authors contributed equally to this work

Correspondence: Xin Zhao; Qiang Li, Email zhaoxin@cque.edu.cn; liqiang19840718@126.com

Objective: The liver protection of blood coral polysaccharide (BCP) was investigated.

Materials and Methods: We evaluated the effect of BCP on liver pathology, liver function, oxidation and inflammation-related indicators of D-Gal/LPS-induced acute liver failure (ALF) mice in vivo.

Results: Liver index and liver pathology observation in mice showed that BCP could inhibit liver tissue swelling and hemorrhage, hepatocyte damage, and inflammatory infiltration in ALF. Serum liver function results showed that BCP effectively inhibits the levels of aspartate aminotransferase (AST), alanine aminotransferase (ALT), lactate dehydrogenase (LDH), total bilirubin (TBil), alkaline phosphatase (AKP), myeloperoxidase (MPO). High dose-blood coral polysaccharide (H-BCP) was better than silymarin. Serum antioxidant and immune results showed that BCP increased the levels of superoxide dismutase (SOD), catalase (CAT), glutathione (GSH), and glutathione peroxidase (GSH-Px), and inhibited the levels of malondialdehyde (MDA) and nitric oxide (NO). Also, BCP increased immunoglobulins G (IgG) and A (IgA) levels, thereby enhancing humoral immunity. Liver anti-inflammatory ELISA results showed that BCP reduced the levels of interleukin (IL)-6, IL-1β, IL-17, tumor necrosis factor (TNF)-α, and interferon (IFN)-γ, and enhanced the level of anti-inflammatory factor IL-10. H-BCP was the most effective treatment. Real-time quantitative reverse transcription-polymerase chain reaction (RT-qPCR) of liver tissues confirmed that BCP increases the relative expression levels of antioxidant and anti-inflammatory-related cuprozinc superoxide dismutase (Cu/Zn-SOD, SOD1), manganese superoxide dismutase (Mn-SOD, SOD2), CAT, GSH, GSH-Px, and IL-10. In contrast, it inhibits inflammation-related genes IL-6, IL-1β, IL-17, TNF-α, IFN-γ, inducible nitric oxide synthase (iNOS, NOS2), and cyclooxygenase (COX)-2. In addition, BCP also inhibits the nuclear factor κ-light-chain-enhancer of activated B cells (NF-κB) and enhance B-cell inhibitor-α (IκB-α) gene relative expression in the liver, which may be related to NF-κB pathway inhibition.

Conclusion: BCP prevents D-Gal/LPS-induced ALF in mice, and its effect is concentration dependent.

Keywords: blood coral polysaccharide, acute liver failure, antioxidant, anti-inflammatory, immunomodulatory

Introduction

Massive hepatocyte necrosis and severe liver dysfunction cause acute liver failure (ALF), often accompanied by hepatic encephalopathy. ALF is most common in young and middle-aged patients with liver disease. The clinical course is progressive multiple organ failure, with rapid onset, poor prognosis, and high mortality. There are no specific treatments, and most of them focus on maintaining the patient's vital functions, expecting liver function recovery, or liver transplantation. Defining ALF pathogenesis and finding effective treatment methods are currently the focus of researchers.[1]

The combined D-galactose/Lipopolysaccharide (D-Gal/LPS) ALF induction model is simple to operate and has good reproducibility, making it the preferred ALF animal model. High levels of D-Gal are converted to aldose and

hydroperoxides catalyzed by galactose oxidase in the liver, generating reactive oxygen species (ROS).[2] In addition, advanced glycation end products (AGEs) formed by the D-Gal reaction in vivo also exacerbate the oxidation process.[3] LPS is a pathogen-associated molecular pattern (PAMP), which mediates the innate immune response and induces inflammatory mediators by activating mononuclear phagocytic system (MPS) release and eventually developing ALF.[4] Most rodents are naturally resistant to LPS, so D-Gal sensitization combined with low-dose LPS is often used to establish an ALF animal model. D-Gal increases mice exacerbation intensity to LPS, which greatly intensifies hepatotoxicity and lethal toxicity of LPS in vivo.[5,6]

Polysaccharides, natural macromolecular carbohydrates with a very complex structure, widely exist in various organisms. In addition to their role as a scaffold, they have an extensive range of biological activities. Due to the special living environments, such as high pressure, high salt, low temperature, hypoxia, and no light, the red algae polysaccharides' synthesis is different from that of terrestrial animals and plants. Moreover, red algae produce polysaccharides with specific structures and physiological characteristics during their growth and metabolism.[7,8] Polysaccharides are the most abundant bioactive component in red algae, including galactan (galactosan), mannan, and xylan in the cell wall and glucan in the cytoplasm. Among them, galactan has the highest content and is the most extensively studied.[9] Red algae polysaccharides are mostly sulfate-rich polysaccharides, and their functions mainly depend on their molecular weight, sulfate group content, monosaccharide composition, and ordering. It exhibits good biological activity in many aspects.[10–13]

Blood coral, a type of red algae that has been shown to antagonize oxidative stress in H9c2 rat heart cells, was used in this study.[14] Mice were fed with blood coral polysaccharides (BCP) to improve their body constitution, and then ALF was induced with D-Gal/LPS) treatment. The ability of BCP to prevent ALF in mice was evaluated by liver function, oxidation, inflammation, and immunity indicators in vivo.

Materials and Methods
Experimental Materials and Reagents
Blood coral was purchased in Beihai Yuzhenduo Food Co., Ltd. (Beihai, Guangxi, China). LPS (from *Escherichia coli* 055: B5) and D-galactose were obtained from Beijing Solarbio Science & Technology Co., Ltd. (Beijing, China).

Preparation of Blood Coral Polysaccharide (BCP)
Blood coral was diluted with double distilled water (ddwater) at 1: 20 (W/V), extracted in a water bath (95°C, 40 min) three times and vacuum filtered to combine the filtrates. The filtrate was suction filtered to remove impurities and then evaporated and concentrated to about 100 mL on a rotary evaporator. Anhydrous ethanol was added to the solution to an 80% final concentration, and the solution was allowed to stand overnight at 4°C. Samples were centrifuged at 4000 r/min for 10 min, and the supernatant was discarded. The precipitate was repeatedly dissolved in hot water (100 mL), precipitated with 80% ethanol (12h), centrifuged (4000 r/min for 10 min at 4°C), and freeze-dried (48 h) to obtain crude polysaccharides. The crude polysaccharides were removed by the *Sevag* method for protein and decolorized activated carbon particles, freeze-dried to obtain the refined blood coral polysaccharide, and cryopreserved until use.

In vivo Liver-Protective Capacity
Experimental mice: forty Kunming male SPF mice (6-week-old) were obtained from Chongqing Ensiweier Biotechnology Co., Ltd. and were adaptively reared in the animal room for 1 week.

Mice grouping and modeling: Forty mice were randomly divided into five groups: (1) no treatment control, (2) the model, (3) silymarin treatment control, (4) low-dose blood coral polysaccharide treatment (L-BCP), and (5) high-dose blood coral polysaccharide treatment (H-BCP). Each group contained eight animals. The modeling operation was as follows: treatment groups were given 0.2 mL of silymarin (100 mg/kg bw)[15] and BCP (150 mg/kg bw and 300 mg/kg bw)[14] by gavage per day, respectively. Other groups were replaced with 0.9% normal saline for 2 weeks. Two weeks later, except the normal group, animals were intraperitoneally injected with 0.2 mL of D-Gal/LPS (300 mg/kg·bw, 30 mg/kg·bw)[16] and fasted for 18 hours to eliminate some components in the diet that may affect the detection indicators, during which time the mice were allowed to drink water and move freely. The composition of mouse diet (mass/%): wheat flour (25), oatmeal (25), corn flour (25), soybean

flour (10), fish meal (8), hog bone powder (4), yeast powder (2), refined salt (1).[17] The D-Gal/LPS-induced ALF model is shown in Figure 1. The protocol for these experiments was approved by the Ethics Committee of Chongqing Collaborative Innovation Center for Functional Food, Chongqing, China, and followed the national standard of the People's Republic of China (GB/T 35892-2018) laboratory animal guidelines for ethical review of animal welfare.

Sample collection: After the mice were weighed, ether anesthetized and blood were collected from retro-orbital plexus, left standing at 4°C for 2h, centrifuged (4°C, 3000 r/min, 10 min), and the serum was obtained (−80°C). After cervical dislocation, the mice were dissected to obtain liver tissue, washed blood with pre-cooled saline, and weighed. Part of the liver was cut for sectioning, and the rest was frozen (−80°C).

Organ index and histological analysis of the liver: liver coefficient was obtained by the formula liver weight (g)/ mouse weight (g) × 100. Part of the liver was fixed with tissue fixative (4% paraformaldehyde, 24 h), embedded in paraffin, stained with hematoxylin–eosin (H&E), observed under a microscope (BX53, Olympus, Tokyo, Japan), and the quantitative analysis method was based on the study of Knodell et al.[18]

Determination of antioxidant, anti-inflammatory, liver function, and immune regulation-related indexes in serum and liver: before detection, the liver (1.0 g) was mixed with pre-cooled normal saline at a mass ratio of 1:9 and then homogenized to obtain the supernatant. Total protein was detected by Coomassie brilliant blue method. Catalase (CAT) activity, glutathione (GSH) content, superoxide dismutase (SOD) activity, glutathione peroxidase (GSH-Px) activity, malondialdehyde (MDA) content, nitric oxide (NO) content, aspartate aminotransferase (AST), alanine aminotransferase (ALT), lactate dehydrogenase (LDH), total bilirubin (TBil), alkaline phosphatase (AKP), and myeloperoxidase (MPO) in serum were performed according to kits (Nanjing Jiancheng Bioengineering Institute, Nanjing, China). Levels of IgG and IgA in serum, and TNF-α, IFN-γ, and IL-1β, IL-6, IL-10, and IL-17 in the liver were examined by enzyme-linked immunosorbent assay (ELISA) kits (Shanghai Enzyme-linked Biotechnology Co., Ltd., Shanghai, China).

qPCR analysis of antioxidant and anti-inflammatory mRNA in the liver of mice: total RNA extraction was performed at 4°C. A mixture of liver tissue (100 mg) and Trizol (1 mL) was homogenized, chloroform (200 μL) was added, and the supernatant was obtained after centrifugation. The supernatant was then mixed with an equal volume of isopropanol for 15 min, centrifuged to obtain a yellow RNA pellet, and washed with 75% ethanol solution (prepared with RNase-Free water). The procedure was repeated 3 times. After washing, the centrifuge tubes containing RNA were air-dried on a clean bench for 3 minutes. After air drying, pellets were diluted with 20 μL RNase-Free water (0.22-μL filter). The RNA concentration and purity were identified by detecting the ratio of A_{260} to A_{280} (if in the range of 1.8–2.0) and then diluted to 1 μg/mL. Reverse transcription was performed according to RevertAid First Stand cDNA Synthesis Kit instructions (Thermo Fisher Scientific). The template and premix (SYBR® Select Master Mix; Thermo Fisher Scientific, Inc., Waltham, MA, USA) systems are mixed and then amplified in an automatic thermalcycler (CFX Connect, Bio-Rad, Hercules, CA, USA). qPCR amplification reaction
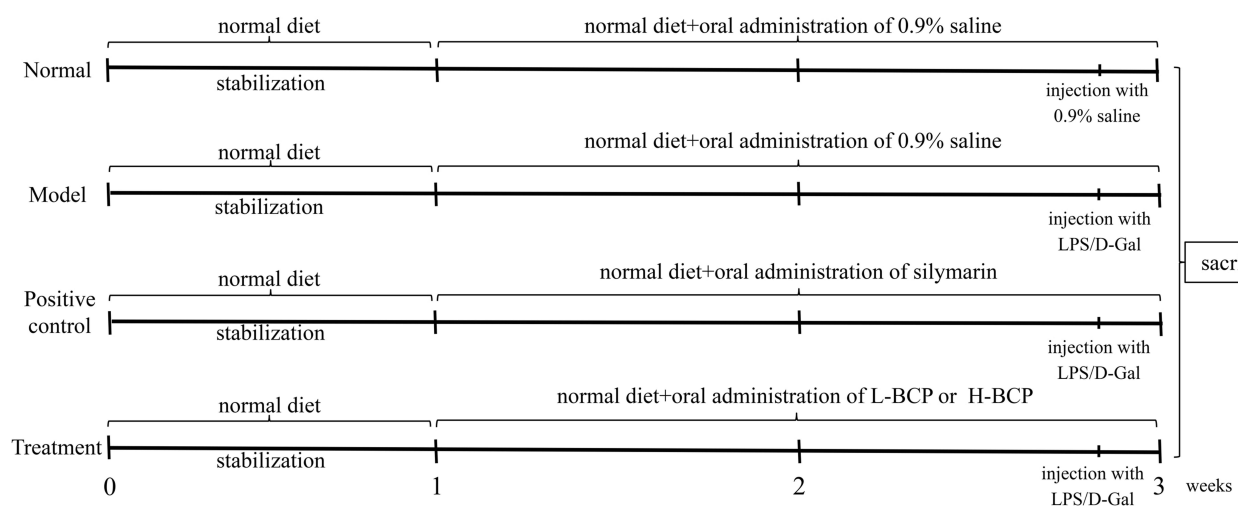

Figure 1 D-Gal/LPS-induced acute liver failure (ALF) model in mice.

was as follows: pre-denaturation: 95°C, 30 seconds; PCR reaction: 95°C, 5 seconds, and 60°C, 30 seconds; 40 cycles. β-Actin served as an internal control, and threshold cycle (C_T) values were analyzed. mRNA expression was analyzed according to formula $2^{-\Delta\Delta Ct}$. All experiments were performed in triplicate. The primers are shown in Table 1.

Statistical Analysis

The experiments were performed in triplicate and expressed as mean ± standard deviation. A $P<0.05$ was considered to be statistically significant. Significant differences between groups were assessed by SPSS software (Chicago, USA), with the Shapiro–Wilk test for data normality and one-way ANOVA and Tukey's test for significance analysis.

Results

Body Weight and Liver Index of Mice

As shown in Table 2, the model mice's body weight, liver weight, and liver index changed significantly ($P < 0.05$), indicating a significant model induction effect. BCP intervention can inhibit the worsening of this condition, while H-BCP is more effective and more similar to silymarin.

Appearance and Histological Analysis of Mice Liver

Figure 2A shows that the normal group livers were bright red, smooth, and soft. In contrast, liver tissues of the D-Gal/LPS-injured mice were dark red and had visible bleeding spots. After silymarin and BCP treatments, the degree of liver color deepening in mice was significantly reduced. The H-BCP and silymarin groups' liver color bleeding was lighter than in the L-BCP group and similar to normal mice.

Liver histopathology was further evaluated by H&E staining (Figure 2B). Hepatic lobules of the normal group had normal structure, the hepatic cord hepatocytes were regularly arranged, the hepatocyte structure was complete without swelling, the size and staining were uniform, the boundaries were orderly and clear, and no inflammatory cell infiltration or necrosis were found. On the contrary, in the model group, hepatocytes were destroyed, the hepatic lobules' arrangement was disordered, large areas of hepatocytes were degenerated and necrotic with uneven staining and unclear boundaries, the nuclei were swollen, fragmented with eosinophilic changes, and the cytoplasm was loose with

Table 1 Primer Sequences

Primer	Forward Primer (3'–5')	Reverse Primer (3–5')
SOD2	5'-CAGACCTGCCTTACGACTATGG-3'	5'-CTCGGTGGCGTTGAGATTGTT-3'
SOD1	5'-AACCAGTTGTGTTGTCAGGAC-3'	5'-CCATGTTTTCTTAGAGTGAGG-3'
GSH-Px	5'-GTCGGTGTATGCCTTCTCGG-3'	5'-AGAGAGACGCGACATTCTCAAT-3'
GSH	5'-TATCAGAGGCGGGAAATCTCTT-3'	5'-ATTCTTGCTTCGGCCACATAC-3'
CAT	5'-GGAGGCGGGAACCCAATAG-3'	5'-GTGTGCCATCTCGTCAGTGAA-3'
IL-6	5'-CTGCAAGAGACTTCCATCCAG-3'	5'-AGTGGTATAGACAGGTCTGTTGG-3'
IL-10	5'-CTTACTGACTGGCATGAGGATCA-3'	5'-GCAGCTCTAGGAGCATGTGG-3'
IL-1β	5'-GAAATGCCACCTTTTGACAGTG-3'	5'-TGGATGCTCTCATCAGGACAG-3'
IL-17	5'-TGAGCTTCCCAGATCACAGA-3'	5'-TCCAGAAGGCCCTCAGACTA-3'
TNF-α	5'-CAGGCGGTGCCTATGTCTC-3'	5'-CGATCACCCCGAAGTTCAGTAG-3'
IFN-γ	5'-GGCCTAGCTCTGAGACAATGAAC-3'	5'-TGACCTCAAACTTGGCAATACTC-3'
IκB-α	5'-CGCGGGATGGCCTCAAGAAGGA-3'	5'-GCCAAGTGCAGGAACGAGTCT-3'
NF-κB	5'-ATGGCAGACGATGATCCCTAC-3'	5'-CGGAATCGAAATCCCCTCTGTT-3'
NOS2	5'-GTTCTCAGCCCAACAATACAAGA-3'	5'-GTGGACGGGTCGATGTCAC-3'
COX2	5'-TTCCAATCCATGTCAAAACCGT-3'	5'-AGTCCGGGTACAGTCACACTT-3'
β-Actin	5'-GGCATCACACTTTCTACAACG-3'	5'-GGCAGGAACATTAAAGGTTTC-3'

Abbreviations: SOD1, Cu/Zn-SOD, cuprozinc-superoxide dismutase; SOD2, Mn-SOD, manganese superoxide dismutase; CAT, catalase; GSH, glutathione; GSH-Px, glutathione peroxidase; IL-6, -10, -17, -1β, interleukin-6, -10, -17, -1β; TNF-α, tumor necrosis factor-α; IFN-γ, interferon-γ; NOS2, iNOS, inducible nitric oxide synthase; COX2, cyclooxygenase-2; NF-Kb, nuclear factor κ-light-chain-enhancer of activated B cells; IκB-α, B-cell inhibitor-α.

Table 2 Effects of Blood Coral Polysaccharides (BCP) on Body Weight, Liver Weight, and Liver Index of Mice Induced by D-Gal/LPS

Group	Body Weight (g)	Liver Weight (g)	Liver Index
Normal	59.84±4.48[a]	1.96±0.27[b]	3.29±0.51[b]
Model	47.19±4.75[b]	2.44±0.14[a]	5.22±0.69[a]
Silymarin	44.20±6.21[bc]	2.20±0.21[ab]	5.09±0.99[a]
L-BCP	39.96±3.31[c]	2.05±0.32[b]	5.15±0.78[a]
H-BCP	41.31±2.16[bc]	2.05±0.22[b]	4.98±0.53[a]

Notes: [a–c]Values presented are the mean ± standard deviation. [a–c]Mean values with different letters in the same row are significantly different ($P < 0.05$) according to Tukey's test. Normal: 0.9% normal saline gavage; Model: intraperitoneal injection of D-Gal/LPS; Silymarin: 100 mg/kg ·bw gavage of silymarin, and intraperitoneal injection of D-Gal/LPS; L-BCP: 150 mg/kg ·bw gavage of blood coral polysaccharides, and intraperitoneal injection of D-Gal/LPS; H-BCP: 300 mg/kg ·bw gavage of blood coral polysaccharides, and intraperitoneal injection of D-Gal/LPS. Organ index (%) = organ weight (g)/body weight of mice (g) ×100.

inflammatory infiltrate. The silymarin- and H-BCP mice hepatocytes recovered order, and the hepatocyte edema, inflammatory infiltration, and cell necrosis were significantly reduced. In L-BCP group, some degeneration of the normal structure of hepatocytes was observed, and a small number of inflammatory cells showed slight morphological changes.

The Biochemical Index Levels in Mice Serum
Model mice serum biochemical markers had statistical differences compared to normal mice (Table 3). D-Gal/LPS treatment significantly increased serum ALT, AST, LDH, Tbil, AKP, and MPO ($P < 0.05$). After silymarin and BCP intervention, ALT, AST, LDH, Tbil, AKP, and MPO decreased significantly ($P < 0.05$), in which L-BCP was the closest overall to the silymarin intervention group, while H-BCP showed a best intervention effect.

The Antioxidant Index of SOD, CAT, GSH, GSH-Px, MDA, and NO Levels in Mice Serum
MDA and NO serum levels in the model group were significantly increased ($P < 0.05$) than in normal mice (Table 4). After the intervention, the serum levels of MDA and NO in the silymarin L-BCP, and H-BCP groups were significantly decreased, and the H-BCP group had the most significant improvement ($P < 0.05$), suggesting that BCP treatment is beneficial to reduce the levels of MDA and NO in mice.

In the model group serum, SOD, GSH-Px, and CAT activities and GSH content were significantly decreased (Table 4, $P < 0.05$) compared to the normal group. After the intervention, the SOD, GSH-Px, CAT, and GSH content in the silymarin, L-BCP, and H-BCP groups serum were increased ($P < 0.05$). The serum activity of SOD, GSH-Px, and CAT in the H-BCP group were 106.77±0.71 U/mL, 69.92±1.91 U/mL, and 32.08±2.98 U/mL, respectively, stronger than other groups. The silymarin group had the highest GSH content, similar to the H-BCP group. The results showed that BCP treatment was beneficial to increase serum SOD, GSH-Px, and CAT activities and GSH content, and H-BCP had a better effect.

The Immunoregulatory Index of IgG and IgA Levels in Mice Serum
After induction, the model serum IgG and IgA immune levels weakened. After BCP treatment, IgG and IgA were significantly increased (Table 5), indicating that the humoral immune function of the mice was significantly improved, and the effect of H-BCP was more effective.

The Anti-Inflammatory Index of IL-6, IL-10, IL-1β, IL 17, TNF-α, and IFN-γ Levels in Mice Liver
To further explore the protective mechanism of BCP on the liver, we examined IL-6, IL-10, IL-1β, IL-17, TNF-α, and IFN-γ associated with inflammation in mouse liver (Table 6). The IL-6, IL-1β, IL-17, TNF-α, and IFN-γ levels in the model group liver were the strongest in silymarin, L-BCP, and H-BCP treatments, inflammatory cytokines were reduced to varying degrees, and the effect in the H-BCP group was better. On the other hand, IL-10 was the highest in normal
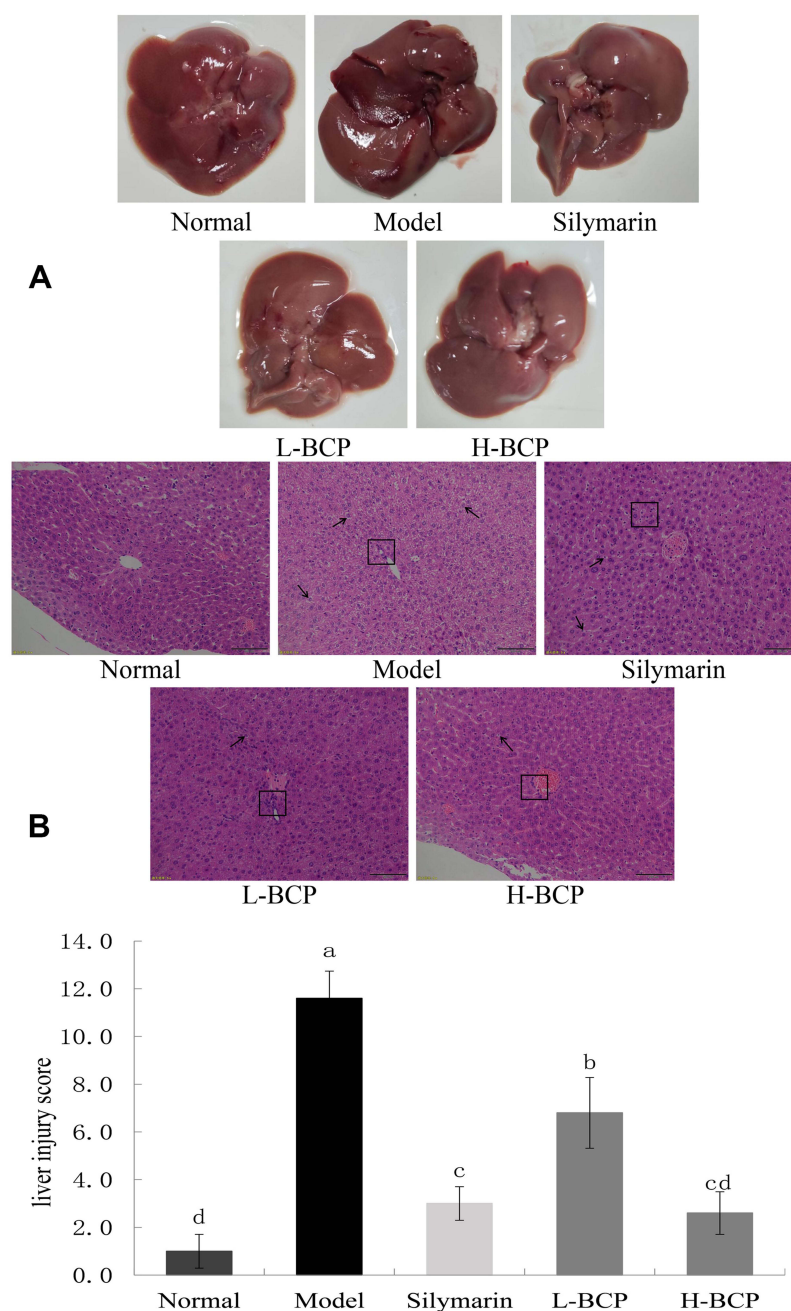
Figure 2 Liver tissue appearance (**A**) and hematoxylin–eosin stain and liver injury score (**B**). [a–d] Mean values with different letters in the same bar graph are significantly different ($P < 0.05$), per Tukey's test. The black arrows in the figure indicates the degree of liver cell looseness and swelling, and the black box indicates liver inflammatory factors. Normal: 0.9% normal saline gavage; Model: intraperitoneal injection of D-Gal/LPS; Silymarin: 100 mg/kg bw gavage of silymarin, and intraperitoneal injection of D-Gal/LPS; L-BCP: 150 mg/kg bw gavage of blood coral polysaccharides, and intraperitoneal injection of D-Gal/LPS; H-BCP: 300 mg/kg bw gavage of blood coral polysaccharides, and intraperitoneal injection of D-Gal/LPS.

liver, significantly decreased ($P < 0.05$) after induction. After silymarin, L-BCP, and H-BCP treatments, IL-10 level was increased again, and it was dose-related, and the therapeutic effect of silymarin was between that of L-BCP and H-BCP.

Antioxidants Relative Gene Expression and Anti-Inflammatory Index in Mice Liver

We also investigated the antioxidant and anti-inflammatory mechanisms of BCP at the gene level by qRT-PCR (Figures 3–5). The relative mRNA abundances of SOD1, SOD2, CAT, GSH, and GSH-Px in normal and post-intervention livers were higher than in the model group. After the intervention, the relative mRNA levels of CAT,

Table 3 The Levels of AST, ALT, LDH, and TBil in the Serum of Mice with Liver Injury Induced by D-Gal/LPS

Group	AST (U/L)	ALT (U/L)	LDH (U/L)	Tbil (μmol/L)	AKP (U/L)	MPO (U/L)
Normal	17.87±0.46[c]	10.92±0.21[cd]	242.03±26.15[c]	3.66±0.16[d]	92.23±10.99[b]	7.45±0.8[d]
Model	28.69±0.81[a]	17.48±0.48[a]	539.35±17.21[a]	13.7±0.34[a]	124.3±215.94[a]	17.54±1.14[a]
Silymarin	20.59±0.77[b]	12.56±0.68[c]	323.24±15.78[bc]	8.92±0.49[bc]	98.7±11.79[b]	14.35±0.56[b]
L-BCP	18.69±0.52[c]	14.59±0.80[b]	352.38±21.02[b]	10.03±0.49[b]	84.91±7.36[bc]	13.16±0.34[b]
H-BCP	13.43±0.65[d]	9.50±0.89[d]	303.97±23.12[bc]	7.95±0.49[c]	70.41±4.59[c]	11.24±0.35[c]

Notes: [a–d]Values presented are the mean ± standard deviation. [a–d]Mean values with different letters in the same row are significantly different (*P* < 0.05) according to Tukey's test. Normal: 0.9% normal saline gavage; Model: intraperitoneal injection of D-Gal/LPS; Silymarin: 100 mg/kg ·bw gavage of silymarin, and intraperitoneal injection of D-Gal/LPS; L-BCP: 150 mg/kg ·bw gavage of blood coral polysaccharides, and intraperitoneal injection of D-Gal/LPS; H-BCP: 300 mg/kg ·bw gavage of blood coral polysaccharides, and intraperitoneal injection of D-Gal/LPS.
Abbreviations: AST, aspartate aminotransferase; ALT, alanine aminotransferase; LDH, lactate dehydrogenase; TBil, total bilirubin; AKP, alkaline phosphatase; MPO, myeloperoxidase.

Table 4 The SOD, CAT, GSH-Px, GSH, MDA, and NO Levels in Serum of Mice with Oxidative Damage Induced by D-Gal/LPS

Group	SOD (U/mL)	GSH-Px (U/mL)	CAT (U/mL)	GSH (μmol/L)	MDA (nmol/mL)	NO (μmol/L)
Normal	104.86±2.78[ab]	53.18±1.60[b]	25.52±2.75[b]	17.97±1.68[a]	4.29±0.25[bc]	2.24±0.05[c]
Model	95.54±2.36[c]	24.83±1.22[e]	16.67±2.65[c]	3.97±1.19[d]	5.58±0.21[a]	3.7±0.24[a]
Silymarin	101.47±1.14[b]	32.81±1.49[d]	31.49±1.21[a]	14.73±1.704[b]	3.53±0.21[c]	1.8±0.03[d]
L-BCP	102.67±1.24[ab]	40.21±1.43[c]	25.12±3.49[b]	9.61±1.77[c]	4.58±0.5[b]	2.93±0.16[b]
H-BCP	106.77±0.71[a]	69.92±1.91[a]	32.08±2.98[a]	12.41±1.65[b]	2.36±0.13[d]	1.41±0.05[e]

Notes: [a–c]Values presented are the mean ± standard deviation. [a–e]Mean values with different letters in the same row are significantly different (*P* < 0.05) according to Tukey's test. Normal: 0.9% normal saline gavage; Model: intraperitoneal injection of D-Gal/LPS; Silymarin: 100 mg/kg ·bw gavage of silymarin, and intraperitoneal injection of D-Gal/LPS; L-BCP: 150 mg/kg ·bw gavage of blood coral polysaccharides, and intraperitoneal injection of D-Gal/LPS; H-BCP: 300 mg/kg ·bw gavage of blood coral polysaccharides, and intraperitoneal injection of D-Gal/LPS.
Abbreviations: SOD, superoxide dismutase; CAT, catalase; GSH, glutathione; GSH-Px, glutathione peroxidase; MDA, malondialdehyde; NO, nitric oxide.

Table 5 The Levels of IgA and IgG in the Serum of Mice Induced by D-Gal/LPS

Group	IgA (μg/mL)	IgG (mg/mL)
Normal	32.85±0.59[a]	3.18±0.03[a]
Model	29.65±0.65[c]	2.68±0.03[d]
Silymarin	33.37±0.10[a]	3.00±0.07[b]
L-BCP	32.09±0.68[b]	2.88±0.01[c]
H-BCP	33.72±0.60[a]	3.01±0.03[b]

Notes: [a–d]Values presented are the mean ± standard deviation. [a–d]Mean values with different letters in the same row are significantly different (*P* < 0.05) according to Tukey's test. Normal: 0.9% normal saline gavage; Model: intraperitoneal injection of D-Gal/LPS; Silymarin: 100 mg/kg ·bw gavage of silymarin, and intraperitoneal injection of D-Gal/LPS; L-BCP: 150 mg/kg ·bw gavage of blood coral polysaccharides, and intraperitoneal injection of D-Gal/LPS; H-BCP: 300 mg/kg ·bw gavage of blood coral polysaccharides, and intraperitoneal injection of D-Gal/LPS.
Abbreviations: IgG, immunoglobulins G; IgA, immunoglobulins A.

GSH, and GSH-Px were between the model and normal groups. Among them, the H-BCP induced effect was stronger than L-BCP, similar to silymarin. Notably, SOD1 and SOD2 relative mRNA increased significantly (*P* < 0.05), even higher than the normal group.

The relative mRNA abundances of IL-6, IL-1β, IL-17, TNF-α, and IFN-γ were the highest in the model group. After silymarin, L-BCP, and H-BCP treatments, the relative expression of inflammatory factors decreased. H-BCP showed the

Table 6 The Levels of IL-6, −10, −1β, −17, TNF-α, and IFN-γ in the Liver of Mice with Inflammation Induced by D-Gal/LPS

Group	IL-6 (pg/ mg prot)	IL-10 (pg/ mg prot)	IL-1β (pg/ mg prot)	IL-17 (pg/mg prot)	TNF-α (pg/ mg prot)	IFN-γ (pg/ mg prot)
Normal	14.81±0.42[bc]	46.62±2.73[a]	17.57±0.21[b]	6.51±0.08[b]	81.28±1.53[bc]	80.41±2.83[b]
Model	17.21±0.18[a]	26.18±1.73[d]	20.86±1.59[a]	7.14±0.18[a]	93.5±3.15[a]	88.99±2.58[a]
Silymarin	14.14±0.16[bc]	37.11±1.69[bc]	15.96±0.82[bc]	6.39±0.3[b]	85.53±2.57[b]	70.56±3.74[c]
L-BCP	15.3±0.6[b]	33.04±0.24[c]	16.15±0.37[bc]	6.37±0.2[b]	82.68±2.08[bc]	80.58±2.97[b]
H-BCP	13.78±0.79[c]	38.18±1.78[b]	14.62±0.39[c]	5.66±0.2[c]	79.15±1.72[c]	72.13±2.88[c]

Notes: [a–d] Values presented are the mean ± standard deviation. [a–d] Mean values with different letters in the same row are significantly different ($P < 0.05$) according to Tukey's test. Normal: 0.9% normal saline gavage; Model: intraperitoneal injection of D-Gal/LPS; Silymarin: 100 mg/kg bw gavage of silymarin, and intraperitoneal injection of D-Gal/LPS; L-BCP: 150 mg/kg bw gavage of blood coral polysaccharides, and intraperitoneal injection of D-Gal/LPS; H-BCP: 300 mg/kg bw gavage of blood coral polysaccharides, and intraperitoneal injection of D-Gal/LPS.
Abbreviations: IL-6, -10, -17, -1β, interleukin-6, -10, -17, -1β; TNF-α, tumor necrosis factor-α; IFN-γ, interferon-γ.

best inhibitory effect, and the L-BCP effect was similar to that of silymarin. On the contrary, the IL-10 mRNA relative abundance in the model group was the lowest and was significantly increased after silymarin, L-BCP, and H-BCP treatments ($P < 0.05$), but were lower than the normal group. Among them, the benefit of H-BCP was superior to that of L-BCP and closer to that of silymarin.

In addition, relative mRNA abundances of IκB-α, NF-κB, NOS2, and COX2 were also examined. BCP inhibited the relative mRNA abundance of NF-κB, NOS2, and COX2 and increased the relative mRNA expression of IκB-α in a dose-dependent manner.

Discussion

During its growth and metabolism, seaweed can produce natural products with specific structures and special physiological activities, such as terpenes, phenols, lipids, polysaccharides, and polypeptides.[19–21] The red algae are widely concerned by scientists because of their wide variety, rich resources, and biological activity.[22] Blood coral is a tropical red alga mainly produced in the South China Sea. Red algae have been shown to contain many bioactive components such as calcium, iron, gum, vitamins, minerals, soluble fiber, and enzymes.[23] Polysaccharides are natural and widely distributed polysaccharide polymer compounds with complex molecular structures and many biological activities. Polysaccharides are the most abundant bioactive components in red algae, and it is mostly composed of sulfated galactosomes, xylan, mannan, and cellulose.[24] Previous studies have shown that galactan (or galactosan), which is alternately linked by α-(1,3) and β-(1,4) glycosidic bonds, is the main monosaccharide component of red algae polysaccharides, is hydrophilic, rich in hydroxyl groups, and easily forms hydrogen bonds between hydroxyl groups. Five monosaccharides were identified from BCP, in which D-galactose had the most content, followed by D- (+)-mannose, D-xylose, D-ribose, D (+)-glucose, consistent with the previous studies.[14,25]

The excessive production of free radicals is the fuse of human aging and various diseases, and people's attention to free radical scavenging continues to rise. Compared with synthetic antioxidants, natural red algae polysaccharides have greater advantages in scavenging free radicals in vitro. Previous studies have shown that *Porphyra yezoensis* polysaccharide has strong scavenging ability to superoxide anion, hydroxyl, and DPPH free radicals.[26] *Gracilaria rubra* agar (GRPS-1-1) was 41.59%, 64.78%, and 59.01% for DPPH, superoxide, and ABTS free radicals, respectively.[27] The study also found that BCP has a strong scavenging ability to DPPH and ABTS free radicals, which is stronger than that of vitamin C at similar concentrations.[14]

We established an ALF mouse model by D-Gal/LPS induction. LPS is the main virulence factor in this model, and large dose of endotoxin into the blood can lead to endotoxemia, endotoxic shock, and multiple organ dysfunction syndrome (MODS). The liver is not only the main organ for removing endotoxin but also one of the target organs most vulnerable to LPS attack.[28] In addition to directly injuring hepatocytes, it can activate various inflammatory cells, mainly Kupffer cells, by binding receptors on the hepatocyte membrane to increase the production of TNF-α, IL-6, and NO.[29] On the one hand, due to the natural resistance of rodents to LPS, individual differences render the liver failure model unstable. On the other hand, single-use of large doses of LPS can cause endotoxemia and lead to liver failure. Therefore,
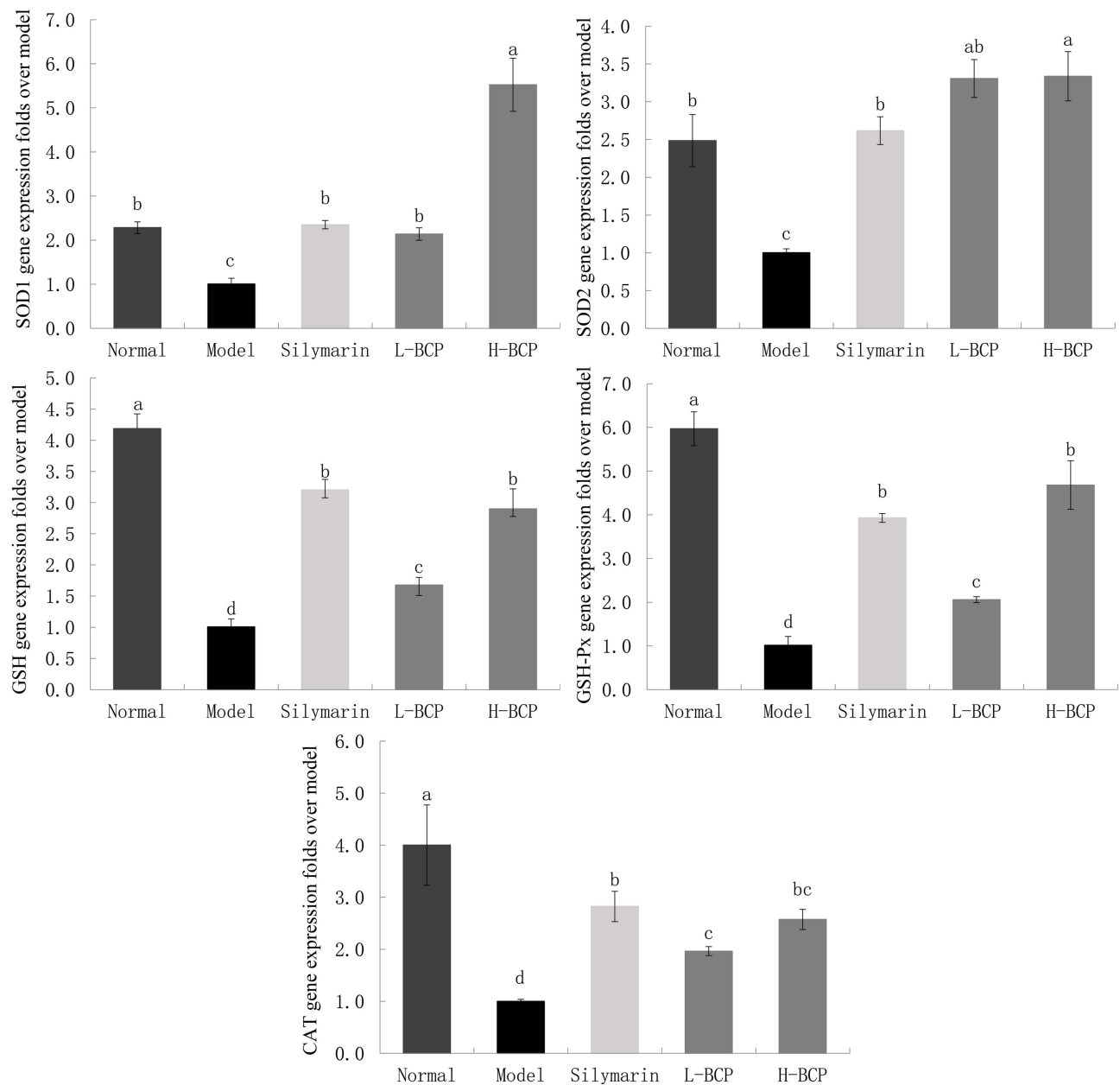
Figure 3 Gene expression of SOD1, SOD2, GSH, GSH-Px, and CAT in the liver. [a–d]Mean values with different letters in the same bar graph are significantly different ($P <$ 0.05), per Tukey's test. Normal: 0.9% normal saline gavage; Model: intraperitoneal injection of D-Gal/LPS; Silymarin: 100 mg/kg bw gavage of silymarin, and intraperitoneal injection of D-Gal/LPS; L-BCP: 150 mg/kg bw gavage of blood coral polysaccharides, and intraperitoneal injection of D-Gal/LPS; H-BCP: 300 mg/kg bw gavage of blood coral polysaccharides, and intraperitoneal injection of D-Gal/LPS.

G-Gal combined with low-dose LPS was used to induce a rodent liver injury model.[30] D-Gal is an interfering agent of uridine triphosphate in hepatocytes. It can cause energy metabolism disorders by depleting uridylic acid in hepatocytes. It can synergize with LPS and increase the sensitivity of the liver to LPS virulence factors.[31] On the other hand, accumulated D-Gal reacts with proteins to form AGEs and cause oxidative stress in vivo, which leads to increased MDA content and decreases SOD and GSH-Px activities.[32,33] Therefore, D-Gal/LPS-induced ALF is frequently used to study its pathogenesis and prevention. This experiment established an ALF model by D-Gal/LPS induction in Kunming mice.

BCP intervention can improve mice's liver pathological changes caused by unreasonable intake of drugs. The increase or decrease in the liver coefficient can reflect liver edema, congestion, or atrophy. It was previously concluded
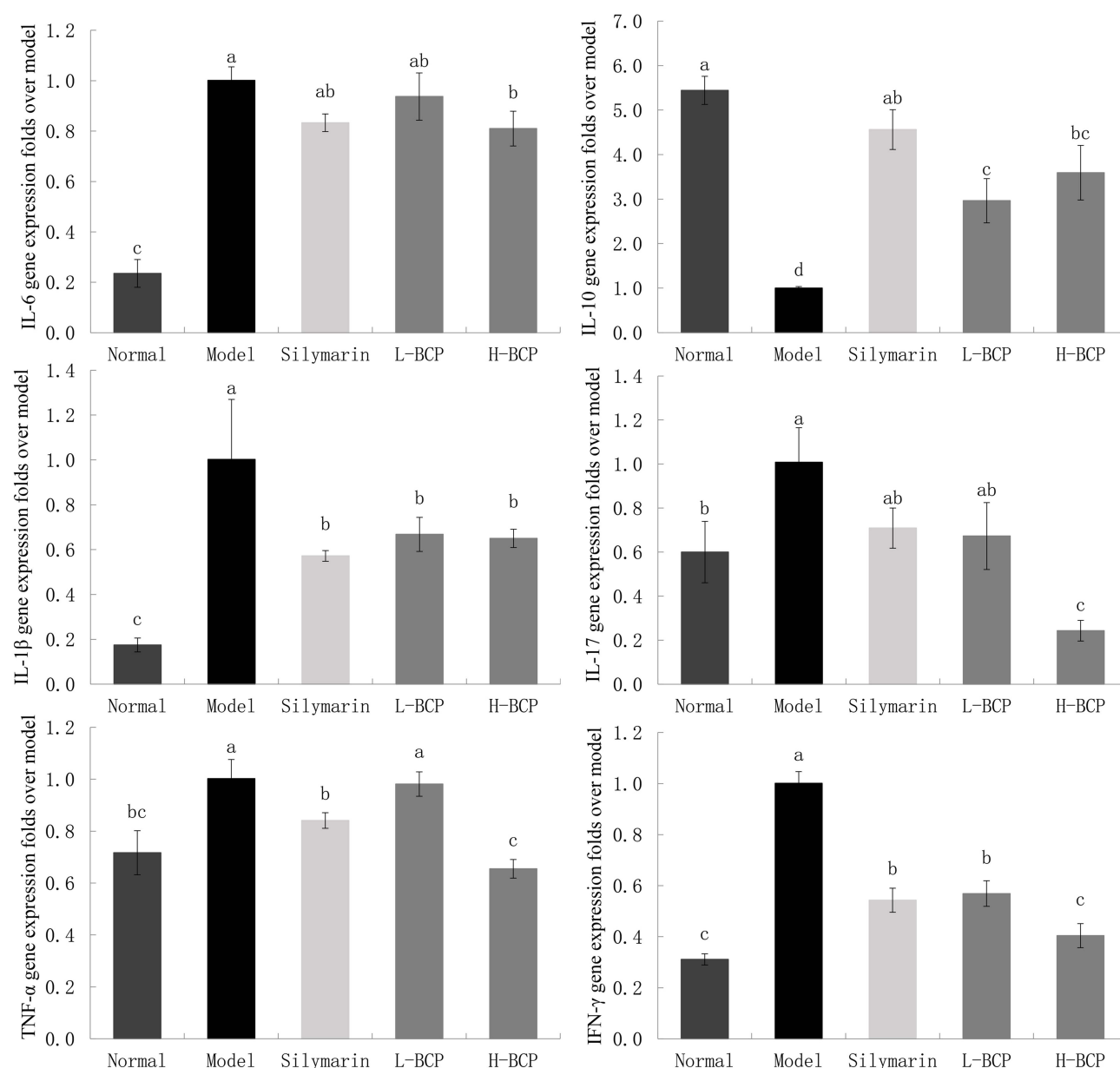
Figure 4 Gene expression of IL-6, −10, −1β, −17, TNF-α, and IFN-γ in the liver. [a–d]Mean values with different letters in the same bar graph are significantly different ($P <$ 0.05), per Tukey's test. Normal: 0.9% normal saline gavage; Model: intraperitoneal injection of D-Gal/LPS; Silymarin: 100 mg/kg ˙bw gavage of silymarin, and intraperitoneal injection of D-Gal/LPS; L-BCP: 150 mg/kg ˙bw gavage of blood coral polysaccharides, and intraperitoneal injection of D-Gal/LPS; H-BCP: 300 mg/kg ˙bw gavage of blood coral polysaccharides, and intraperitoneal injection of D-Gal/LPS.

that D-Gal/LPS-induced acute liver injury could cause liver edema.[34] After dissection of the liver, liver edema, increased liver weight, dark red color with congestion were observed. The damaged liver coefficient increased by 58.6% compared to the normal liver. In comparison, the liver coefficients of the silymarin and BCP intervention groups decreased in different degrees. Pathological analysis showed disordered hepatocyte structure, swollen cells, fragmented nucleus and cytoplasm, multifocal inflammatory cell infiltration in hepatic lobules, eosinophilic enhancement, and coagulative necrosis. The survival status of hepatocytes in the silymarin and BCP intervention groups was significantly improved, similar to the normal liver.

BCP exerts liver protection by enhancing antioxidant activity and inhibiting superoxide production in mice. Studies have shown that the pathogenesis of ALF is variable, but oxidative stress is always indispensable. The imbalance of the body's oxidative and antioxidant systems in D-Gal/LPS-induced ALF leads to oxidative damage to the liver.[35] SOD
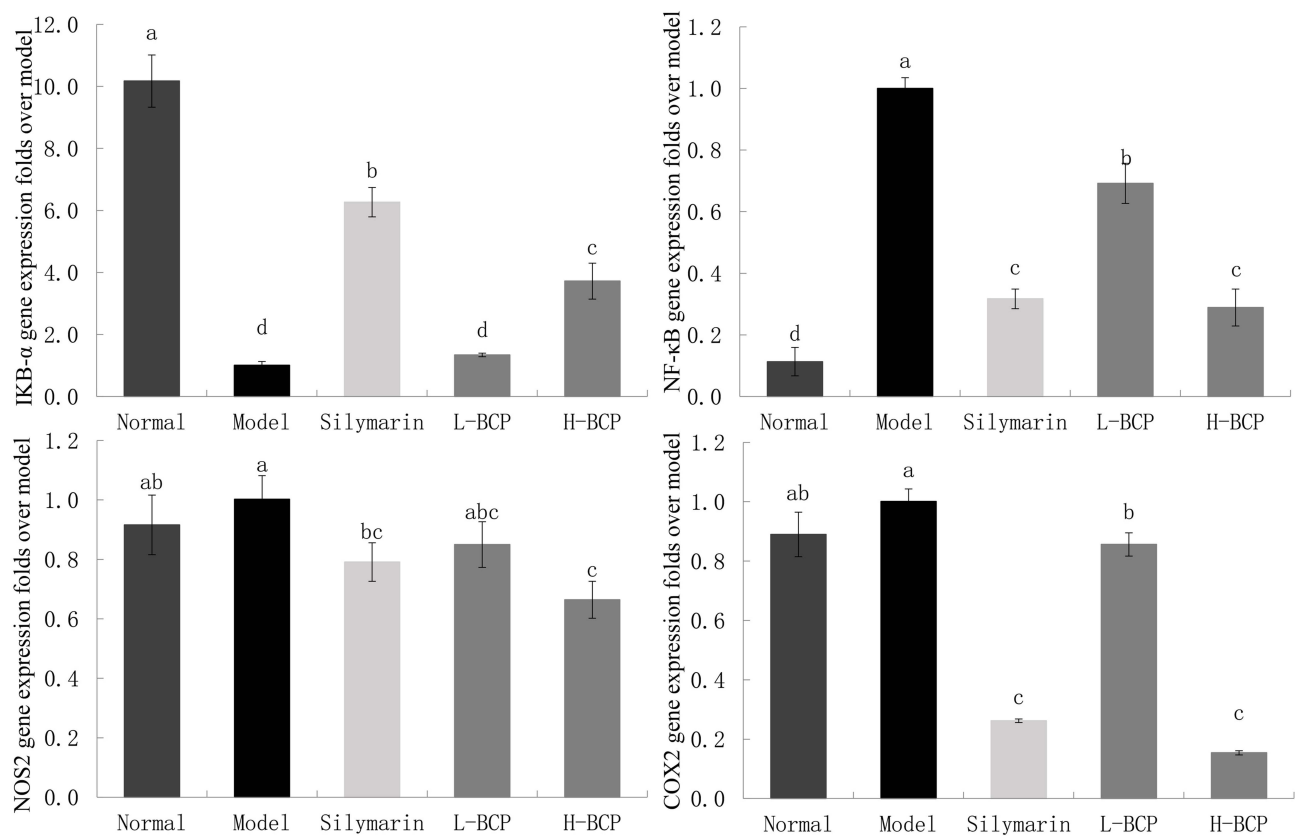
Figure 5 Gene expression of IKB-α, NF-kB, NOS2, and COX2 in the liver. [a–d] Mean values with different letters in the same bar graph are significantly different ($P < 0.05$), per Tukey's test. Normal: 0.9% normal saline gavage; Model: intraperitoneal injection of D-Gal/LPS; Silymarin: 100 mg/kg·bw gavage of silymarin, and intraperitoneal injection of D-Gal/LPS; L-BCP: 150 mg/kg·bw gavage of blood coral polysaccharides, and intraperitoneal injection of D-Gal/LPS; H-BCP: 300 mg/kg·bw gavage of blood coral polysaccharides, and intraperitoneal injection of D-Gal/LPS.

promotes the balance of the oxidation-antioxidation system, catalyzes the dismutation of superoxide to produce hydrogen peroxide, and prevents oxygen toxicity.[36] The high catalase concentration in the liver catalyzes the disproportion of H_2O_2 and inhibits the generation of hydroxyl radicals that are harmful to the body.[37] GSH and its enzymes play a regulatory role in the body's scavenging of free radicals, anti-oxidative damage, and detoxification, and GSH-Px and CAT have a synergistic effect of promoting the decomposition of H_2O_2.[38–40] On the other hand, MDA and NO play important roles in liver oxidative damage. MDA is widely used as a marker of oxidative stress, and D-gal/LPS can induce the body to produce excessive ROS and cause liver peroxidation.[41,42] NO is a chemically active substance rapidly converted to NO_2^- and NO_3^- in the body and activates guanylate cyclase GC and relaxes smooth muscle. NO reacts with ROS aggravating oxidative damage and with superoxide anion forming peroxynitrite, activates NF-κB, and promote Kupffer cells to produce TNF-α.[43]*Blood cora* polysaccharides could inhibit hydrogen peroxide-induced oxidative damage in H9c2 rat cardiomyocytes in vitro by reducing LDH and MDA and enhancing SOD, CAT and GSH levels.[14] In this experiment, BCP could protect mice's liver by down-regulating the contents of MDA and NO, and up-regulating the activity levels of endogenous antioxidant enzymes such as SOD, CAT, GSH-Px, and GSH.

BCP exerts liver protection in mice through anti-inflammatory effects in vivo. The key mechanism of LPS/D-Gal-induced ALF lies in the massive release of various inflammatory substances represented by TNF-α, IL-6, and IL-1β.[44] Research on the pathogenic mechanism of endotoxin has shown that the inflammatory cytokines induced by endotoxin far exceed the direct impact of endotoxin itself on the body, among which TNF-α is the most important and plays a central role in producing other inflammatory cytokines.[45–47] It was shown that LPS treatment of D-Gal-sensitized mice induces a pathological response to ALF characterized by apoptosis, which can be prevented by anti-TNF-α antibody treatment.[48] IL-17 induces early inflammation and amplifies the inflammatory response, acting through the MAP kinase

and the NF-κB pathways. Th17 cells can secrete IL-17, IL-6, and TNF-α, neutrophils activating cytokines, thereby effectively mediating tissue inflammatory response.[49] IL-10 is an inflammatory and immunosuppressive factor that reduces antigen presentation and costimulatory molecules, down-regulates T lymphocyte activity, enhances B cell proliferation and antibody secretion and blocks NF-κB activity.[50] Type II IFNs (IFN-γ in humans) bind to IFN-γ receptor complexes and are involved in immune and inflammatory. When Th1 cells release type II IFN, leukocytes move to the infected tissue, leading to inflammation.[51] The anti-inflammatory effect of red algae is probably related to their sulfated polysaccharides. D2-polysaccharide from *Pyropia yezoensis* has the highest inhibitory effect on Tnf-α secretion in LPS-stimulated RAW264.7 cells, and D3- and D4-polysaccharides were almost inactive. It was speculated that molecular size determines the anti-inflammatory strength of polysaccharides based on degradation experiments.[52] This study also indicated that the inflammatory response was the main factor leading to LPS/D-Gal-induced ALF. IL-1β, IL-6, and TNF-α determine the occurrence and development of ALF, but BCP pretreatment suppressed their increase. At present, there is no clear conclusion about the relationship between the sulfate groups in red algae polysaccharides and inflammation. However, the carboxylic acid moiety acts as an anti-inflammatory agent in common anti-inflammatory drugs, such as aspirin. It can be speculated that the anti-inflammatory mechanism of red algae polysaccharides may be that the acidic polysaccharide fragments generated by its degradation in vivo bind to inflammation-related receptors, thereby partially inhibiting or blocking the expression of inflammatory factors.

BCP exerts liver protection in mice through immunomodulatory effects in vivo. Immunoglobulins (Ig) are mainly present in the extracellular fluid and can recognize and neutralize bacteria, viruses, and other pathogens. They uniquely recognize a specific foreign molecule, an antigen, through its variable region.[53] The core job of the humoral immune system is to produce antibodies, which can work with the complement system in the serum to directly destroy foreign targets.[54] The immunomodulatory activity of red algae polysaccharides has been shown to promote the proliferation and activity of immune cells in vitro. In vivo can stimulate the body's immune response to enhance the effect of immunity.[55,56] After silymarin and BCP interventions, the components with immunomodulatory activity in BCP can also stimulate the body's immune response to promote immune cells proliferation, increase IgG and IgA content, and improve humoral immune function.

Furthermore, BCP exhibited similar antioxidant and anti-inflammatory activities in D-Gal/LPS-induced ALF at the genetic level. In most cells, NF-κB binds to its inhibitory protein IκB family members and exists as an inactive complex in the cytoplasm. Once stimulated by LPS bacteria and their products, activated inflammatory cytokines (eg, TNF-α), dissociate from IκB and transfer into the nucleus to combine with a specific promoter to regulate gene expression. Activated NF-κB promotes transcription and secretion of inflammatory mediators, and participates in physiological and pathological regulatory processes. It has a wide range of effects on diseases and is the main target for drug development.[57] Other studies have shown that red microalga polysaccharides have anti-inflammatory effects in TNF-α-stimulated coronary endothelial cells by significantly inhibiting NF-κB activation.[58] In addition, D-Gal/LPS can induce iNOS expression, promoting large amounts of NO production. NO can produce highly toxic oxidative nitrite with superoxide, resulting in cell neurotoxicity. Furthermore, NO and NF-κB activation are closely related.[59] COX generally has two isomers, COX1 and COX2. Simultaneously, COX2 increases due to inflammatory stimuli and releases the pro-inflammatory factor PGE, causing immune inflammation in the central nervous system, and COX2 and iNOS show a synergistic effect in some pathological aspects.[60] In this experiment, BCP up-regulated Cu/Zn-SOD, Mn-SOD, GSH-Px, GSH, and CAT against hepatic oxidative damage. In addition, BCP inhibited NF-κB activation, thereby inhibiting the expression of a series of inflammatory factors, which may be related to the NF-κB signaling pathway.

Conclusions

BCP can inhibit D-Gal/LPS-induced ALF in mice through antioxidant, anti-inflammatory, and immunomodulatory activities and has good application potential.

Data Sharing Statement

The original contributions presented in the study are included in the article; further inquiries can be directed to the corresponding author/s.

Acknowledgment

Funding

Disclosure

The authors report no conflicts of interest in relation to this work.

References

1. Liu Q. Role of cytokines in the pathophysiology of acute on-chronic liver failure. *Blood Purif*. 2009;28(4):331–341. doi:10.1159/000232940
2. Wu D, Lu J, Zheng Y, Zhou Z, Shan Q, Ma D. Purple sweet potato color repairs D-galactose-induced spatial learning and memory impairment by regulating the expression of synaptic proteins. *Neurobiol Learn Mem*. 2008;90(1):19–27. doi:10.1016/j.nlm.2008.01.010
3. Bucala R, Cerami A. Advanced glycosylation: chemistry, biology, and implications for diabetes and aging. *Adv Pharmacol*. 1992;23:1–34.
4. Remick D, Ward P. Evaluation of endotoxin models for the study of sepsis. *Shock*. 2005;24(Supplement 1):7–11. doi:10.1097/01.shk.0000191384.34066.85
5. Liu X, Robinson D, Veach R, et al. Peptide-directed suppression of a pro-inflammatory cytokine response. *J Biol Chem*. 2000;275 (22):16774–16778. doi:10.1074/jbc.C000083200
6. Kosai K, Matsumoto K, Funakoshi H, Nakamura T. Hepatocyte growth factor prevents endotoxin-induced lethal hepatic failure in mice. *Hepatology*. 1999;30(1):151–159. doi:10.1002/hep.510300102
7. Jha R, Xu Z. Biomedical compounds from marine organisms. *Mar Drugs*. 2004;2(3):123–146. doi:10.3390/md203123
8. Cui Y, Liu X, Li S, et al. Extraction, characterization and biological activity of sulfated polysaccharides from seaweed Dictyopteris divaricata. *Int J Biol Macromol*. 2018;117:256–263. doi:10.1016/j.ijbiomac.2018.05.134
9. Zhong Q, Wei B, Wang S, et al. The antioxidant activity of polysaccharides derived from marine organisms: an overview. *Mar Drugs*. 2019;17 (12):674. doi:10.3390/md17120674
10. Fleita D, El-Sayed M, Rifaat D. Evaluation of the antioxidant activity of enzymatically-hydrolyzed sulfated polysaccharides extracted from red algae; Pterocladia capillacea. *LWT-Food Sci Technol*. 2015;63(2):1236–1244. doi:10.1016/j.lwt.2015.04.024
11. Assreuy A, Gomes D, da Silva S, et al. Biological effects of a sulfated-polysaccharide isolated from the marine red algae champia feldmannii. *Biol Pharm Bull*. 2008;31(4):691–695. doi:10.1248/bpb.31.691
12. da Silva Chagas F, Lima G, Dos Santos V, et al. Sulfated polysaccharide from the red algae Gelidiella acerosa: anticoagulant, antiplatelet and antithrombotic effects. *Int J Biol Macromol*. 2020;159:415–421. doi:10.1016/j.ijbiomac.2020.05.012
13. Khotimchenko M, Tiasto V, Kalitnik A, et al. Antitumor potential of carrageenans from marine red algae. *Carbohydr Polym*. 2020;246:116568. doi:10.1016/j.carbpol.2020.116568
14. Jiang Y, Zhou W, Zhang X, Wang Y, Yang D, Li S. Protective effect of blood cora polysaccharides on H9c2 rat heart cells injury induced by oxidative stress by activating Nrf2/HO-1 signal pathway. *Front Nutritr*. 2021;8:73. doi:10.3389/fnut.2021.632161
15. Sasu A, Herman H, Folk A, et al. Protective effects of silymarin on epirubicin -induced hepatotoxicity in mice. *Stud Univ Vasile Goldis Arad Ser Stiint Vietii*. 2016;26:305.
16. Pu Y, Yang Z, Mo X. Protective effect of luteolin on D-Galactosamine(D-Gal)/Lipopolysaccharide (LPS) induced hepatic injury by in mice. *Biomed Res Int*. 2021;2021:2252705. doi:10.1155/2021/2252705
17. Li C, He Y, Yang Y, et al. Antioxidant and inflammatory effects of Nelumbo nucifera gaertn. *Leaves Oxid Med Cell Longev*. 2021;2021:8375961.
18. Knodell R, Ishak K, Black W, et al. Formulation and application of a numerical scoring system for assessing histological activity in asymptomatic chronic active hepatitis. *Hepatology*. 1981;1(5):431–435. doi:10.1002/hep.1840010511
19. Carson M, Clarke S. Bioactive compounds from marine organisms: potential for bone growth and healing. *Mar Drugs*. 2018;16(9):340. doi:10.3390/md16090340
20. Carte B. Biomedical potential of marine natural products. *Bioscience*. 1996;46:271–286.
21. Jayawardena T, Wang L, Sanjeewa K, Kang S, Lee J, Jeon Y. Antioxidant potential of sulfated polysaccharides from Padina boryana; Protective effect against oxidative stress in in vitro and in vivo zebrafish model. *Mar Drugs*. 2020;18(4):212. doi:10.3390/md18040212
22. Dhargalkar V, Verlecar X. Southern Ocean seaweeds: a resource for exploration in food and drugs. *Aquaculture*. 2009;287(3–4):229–242. doi:10.1016/j.aquaculture.2008.11.013
23. Rodrigues D, Freitas A, Pereira L, et al. Chemical composition of red, brown and green macroalgae from Buarcos bay in Central West Coast of Portugal. *Food Chem*. 2015;183:197–207. doi:10.1016/j.foodchem.2015.03.057
24. Zhou F, Tang H, Sun H, Zheng Z, Ouyang J. Progress in biotransformation of red algal polysaccharides for industrial utilization. *Food Sci*. 2021;42:326–334.
25. O' Sullivan L, Murphy B, McLoughlin P, et al. Prebiotics from marine macroalgae for human and animal health applications. *Mar Drugs*. 2010;8 (7):2038–2064. doi:10.3390/md8072038
26. Wang F, Kong L, Xie Y, et al. Purification, structural characterization, and biological activities of degraded polysaccharides from Porphyra yezoensis. *J Food Biochem*. 2021;45:e13661. doi:10.1111/jfbc.13661
27. Di T, Chen G, Sun Y, Ou S, Zeng X, Ye H. Antioxidant and immunostimulating activities in vitro of sulfated polysaccharides isolated from Gracilaria rubra. *J Funct Foods*. 2017;28:64–75. doi:10.1016/j.jff.2016.11.005

28. Betrapally N, Gillevet P, Bajaj J. Gut microbiome and liver disease. *Transl Res*. 2017;179:49–59. doi:10.1016/j.trsl.2016.07.005

29. Wang J, Wang H, Li L, et al. Development of a rat model of D-galactosamine/lipopolysaccharide induced hepatorenal syndrome. *World J Gastroenterol*. 2015;21(34):9927–9935. doi:10.3748/wjg.v21.i34.9927

30. Zhu Y, Tian D. Experimental research of the effect of endotoxin on glucose metabolism in SD rats model with acute hepatic failure. *J Intern Intensive Med*. 2006;12:119–121.

31. Kemelo M, Wojnarova L, Canová N, Farghali H. D-galactosamine/lipopolysaccharide-induced hepatotoxicity downregulates sirtuin 1 in rat liver: role of sirtuin 1 modulation in hepatoprotection. *Physiol Res*. 2014;63:615. doi:10.33549/physiolres.932761

32. Singh R, Barden A, Mori T, Beilin L. Advanced glycation end-products: a review. *Diabetologia*. 2001;44(2):129–146. doi:10.1007/s001250051591

33. Yamagishi S, Matsui T. Advanced glycation end products, oxidative stress and diabetic nephropathy. *Oxid Med Cell Longev*. 2010;3(2):101–108. doi:10.4161/oxim.3.2.11148

34. Bernal W, Auzinger G, Dhawan A, Wendon J. Acute liver failure. *Lancet*. 2010;376(9736):190–201. doi:10.1016/S0140-6736(10)60274-7

35. Butterfield D, Castegna A, Pocernich C, Drake J, Scapagnini G, Calabrese V. Nutritional approaches to combat oxidative stress in Alzheimer's disease. *J Nutr Biochem*. 2002;13(8):444–461. doi:10.1016/S0955-2863(02)00205-X

36. Zelko I, Mariani T, Folz R. Superoxide dismutase multigene family: a comparison of the CuZn-SOD (SOD1), Mn-SOD (SOD2), and EC-SOD (SOD3) gene structures, evolution, and expression. *Free Radic Biol Med*. 2002;33(3):337–349. doi:10.1016/S0891-5849(02)00905-X

37. Tehrani H, Moosavi-Movahedi A. Catalase and its mysteries. *Prog Biophys Mol Biol*. 2018;140:5–12. doi:10.1016/j.pbiomolbio.2018.03.001

38. Farghali H, Černý D, Kameníková L, et al. Resveratrol attenuates lipopolysaccharide-induced hepatitis in D-galactosamine sensitized rats: role of nitric oxide synthase 2 and heme oxygenase-1. *Nitric Oxide*. 2009;21(3–4):216–225. doi:10.1016/j.niox.2009.09.004

39. Lian L, Wu Y, Wan Y, Li X, Xie W, Nan J. Anti-apoptotic activity of gentiopicroside in d-galactosamine/lipopolysaccharide-induced murine fulminant hepatic failure. *Chem Biol Interact*. 2010;188(1):127–133. doi:10.1016/j.cbi.2010.06.004

40. Ma X, Deng D, Chen W. Inhibitors and Activators of SOD, GSH-Px, and CAT. *Enzyme Inhib Activatators*. 2017;29:207–224.

41. Cui X, Gong J, Han H, et al. Relationship between free and total malondialdehyde, a well-established marker of oxidative stress, in various types of humans biospecimens. *J Thorac Dis*. 2018;10(5):3088. doi:10.21037/jtd.2018.05.92

42. Mohamadi-Zarch S, Baluchnejadmojarad T, Nourabadi D, Khanizadeh A, Roghani M. Protective effect of diosgenin on LPS/D-Gal-induced acute liver failure in C57BL/6 mice. *Microb Pathog*. 2020;146:104243. doi:10.1016/j.micpath.2020.104243

43. Choi W, Shin P, Lee J, Kim G. The regulatory effect of veratric acid on NO production in LPS-stimulated RAW264.7 macrophage cells. *Cell Immunol*. 2012;280(2):164–170. doi:10.1016/j.cellimm.2012.12.007

44. Josephs M, Bahjat F, Fukuzuka K, et al. Lipopolysaccharide and D-galactosamine-induced hepatic injury is mediated by TNF-α and not by Fas ligand. *Am J Physiol Regul Integr Comp Physiol*. 2000;278:R1196–R1201. doi:10.1152/ajpregu.2000.278.5.R1196

45. Silverstein R. D-galactosamine lethality model: scope and limitations. *J Endotoxin Res*. 2004;10(3):147–162. doi:10.1179/096805104225004879

46. Nowak M, Gaines G, Rosenberg J, et al. LPS-induced liver injury ind-galactosamine-sensitized mice requires secreted TNF-α and the TNF-p55 receptor. *Am J Physiol Regul Integr Comp Physiol*. 2000;278:R1202–R1209. doi:10.1152/ajpregu.2000.278.5.R1202

47. Lyu Z, Ji X, Chen G, An B. Atractylodin ameliorates lipopolysaccharide and d-galactosamine-induced acute liver failure via the suppression of inflammation and oxidative stress. *Int Immunopharmacol*. 2019;72:348–357. doi:10.1016/j.intimp.2019.04.005

48. Kuhla A, Eipel C, Abshagen K, Siebert N, Menger M, Vollmar B. Role of the perforin/granzyme cell death pathway in D-Gal/LPS-induced inflammatory liver injury. *Am J Physiol Gastrointest Liver Physiol*. 2009;296:G1069–G1076. doi:10.1152/ajpgi.90689.2008

49. Beringer A, Miossec P. Systemic effects of IL-17 in inflammatory arthritis. *Nat Rev Rheumatol*. 2019;15(8):491–501. doi:10.1038/s41584-019-0243-5

50. Han H, Ma Q, Li C, et al. Profiling serum cytokines in COVID-19 patients reveals IL-6 and IL-10 are disease severity predictors. *Emerg Microb Infect*. 2020;9(1):1123–1130. doi:10.1080/22221751.2020.1770129

51. Karki R, Sharma B, Tuladhar S, et al. Synergism of TNF-α and IFN-γ triggers inflammatory cell death, tissue damage, and mortality in SARS-CoV-2 infection and cytokine shock syndromes. *Cell*. 2021;184(1):149–168. doi:10.1016/j.cell.2020.11.025

52. Yanagido A, Ueno M, Jiang Z, et al. Increase in anti-inflammatory activities of radical-degraded porphyrans isolated from discolored nori (Pyropia yezoensis). *Int J Biol Macromol*. 2018;117:78–86. doi:10.1016/j.ijbiomac.2018.05.146

53. Litman G, Rast J, Shamblott M, et al. Phylogenetic diversification of immunoglobulin genes and the antibody repertoire. *Mol Biol Evol*. 1993;10(1):60–72. doi:10.1093/oxfordjournals.molbev.a040000

54. Keusch G. The history of nutrition: malnutrition, infection and immunity. *J Nutr*. 2003;133(1):336S–340S. doi:10.1093/jn/133.1.336S

55. Zhao X, Jiao G, Yang Y, et al. Structure and immunomodulatory activity of a sulfated agarose with pyruvate and xylose substitutes from Polysiphonia senticulosa Harvey. *Carbohydr Polym*. 2017;176:29–37. doi:10.1016/j.carbpol.2017.08.065

56. Han J, Liu B, Liu Q, et al. Red algae sulfated polysaccharides effervescent tablets attenuated ovalbumin-induced anaphylaxis by upregulating regulatory T cells in mouse models. *J Agric Food Chem*. 2019;67(43):11911–11921. doi:10.1021/acs.jafc.9b03132

57. Tang J, Xu L, Zeng Y, Gong F. Effect of gut microbiota on LPS-induced acute lung injury by regulating the TLR4/NF-kB signaling pathway. *Int Immunopharmacol*. 2021;91:107272. doi:10.1016/j.intimp.2020.107272

58. Levy-Ontman O, Huleihel M, Hamias R, Wolak T, Paran E. An anti-inflammatory effect of red microalga polysaccharides in coronary artery endothelial cells. *Atherosclerosis*. 2017;264:11–18. doi:10.1016/j.atherosclerosis.2017.07.017

59. Paixão J, Dinis T, Almeida L. Malvidin-3-glucoside protects endothelial cells up-regulating endothelial NO synthase and inhibiting peroxynitrite-induced NF-kB activation. *Chem Biol Interact*. 2012;199(3):192–200. doi:10.1016/j.cbi.2012.08.013

60. Appleton I, Tomlinson A, Willoughby D. Induction of cyclo-oxygenase and nitric oxide synthase in inflammation. *Adv Pharmacol*. 1996;35:27–77. doi:10.1016/s1054-3589(08)60274-4